Muon spin relaxation study of $LaTiO_3$ and $YTiO_3$

2008 J. Phys.: Condens. Matter 20 465203

(http://iopscience.iop.org/0953-8984/20/46/465203)

J. Phys.: Condens. Matter **20** (2008) 465203 (7pp) doi:10.1088/0953-8984/20/46/465203

Muon spin relaxation study of $LaTiO_3$ and $YTiO_3$

P J Baker[1], T Lancaster[1], S J Blundell[1], W Hayes[1], F L Pratt[2], M Itoh[3], S Kuroiwa[4] and J Akimitsu[4]

[1] Department of Physics, Oxford University, Parks Road, Oxford OX1 3PU, UK
[2] ISIS Muon Facility, Rutherford Appleton Laboratory, Harwell Science and Innovation Campus, Didcot OX11 0QX, UK
[3] Department of Physics, Nagoya University, Nagoya 464-8602, Japan
[4] Department of Physics and Mathematics, Aoyama Gakuin University, Sagamihara, Kanagawa 229-8558, Japan

E-mail: p.baker1@physics.ox.ac.uk

Received 29 April 2008, in final form 8 July 2008
Published 21 October 2008
Online at stacks.iop.org/JPhysCM/20/465203

Abstract

We report muon spin relaxation (μSR) measurements on two Ti^{3+} containing perovskites, $LaTiO_3$ and $YTiO_3$, which display long-range magnetic order at low temperature. For both materials, oscillations in the time dependence of the muon polarization are observed which are consistent with three-dimensional magnetic order. From our data we identify two magnetically inequivalent muon stopping sites. The μSR results are compared with the magnetic structures of these compounds previously derived from neutron diffraction and μSR studies on structurally similar compounds.

(Some figures in this article are in colour only in the electronic version)

1. Introduction

Despite their structural simplicity (exemplified in figure 1) perovskite compounds of the form ABX_3 show a wide variety of physical properties, particularly when the simple cubic structure is distorted [1]. Changing the ionic radius of the ion on the A-site allows the distortion to be controlled and, through this, the physics of these materials can be tuned [2]. An example of two similar compounds where a small change in the ionic radius causes a significant change in the physical properties is the pair $LaTiO_3$ and $YTiO_3$.

These two compounds are Mott–Hubbard insulators but retain the orbital degree of freedom in the t_{2g} state [3] and show a strong coupling between spin and orbital degrees of freedom [4]. Orbital degeneracy, which can lead to phenomena such as colossal magnetoresistance [5] or unconventional superconductivity [6], is present in isolated Ti t_{2g} ions, but is lifted in these compounds [4]. The size of the A^{3+} ion provides one means of tuning the properties of these titanates [4], affecting the Ti–O–Ti bond angles and exchange interactions. This is evident in the difference between the low-temperature magnetic structures of these two compounds, observed using neutron diffraction [7–9]. $LaTiO_3$ is a G-type antiferromagnet [7, 8], with moments aligned along either the a- or c-axis. The precise value of T_N is very sensitive to the oxygen stoichiometry and reports vary between 120 and ~150 K [10]. $YTiO_3$ orders ferromagnetically [9] with the spins aligned along the c-axis at $T_C = 27$ K; however, there is a G-type antiferromagnetic component along a, and an A-type component along b (see figure 1).

Evidence of orbital excitations due to fluctuations of orbital-exchange bonds has been found in $LaTiO_3$ and $YTiO_3$ using Raman scattering, and these excitations are remarkably similar to the exchange-bond fluctuations which give rise to magnetic Raman scattering in cuprates [10]. A broad range of measurements has demonstrated the underlying orbital ordering in both compounds [2, 8, 12–15], strongly excluding the orbital liquid picture hypothesized for $LaTiO_3$ [16] and agreeing with the reduced orbital moment found in x-ray and NMR measurements on $LaTiO_3$ [7, 17]. It has been shown [18] that the $Y_{1-x}La_xTiO_3$ system is an itinerant-electron antiferromagnet with no orbital ordering for $x > 0.7$ and that an intermediate phase exists for $0.3 < x < 0.7$, with orbital-order fluctuations and ferromagnetic interactions that reduce T_N. For $x < 0.3$ the system shows orbital ordering and a ferromagnetic transition and it was suggested that even at $x = 0$ the volume of the orbitally ordered region does not encompass the whole sample.

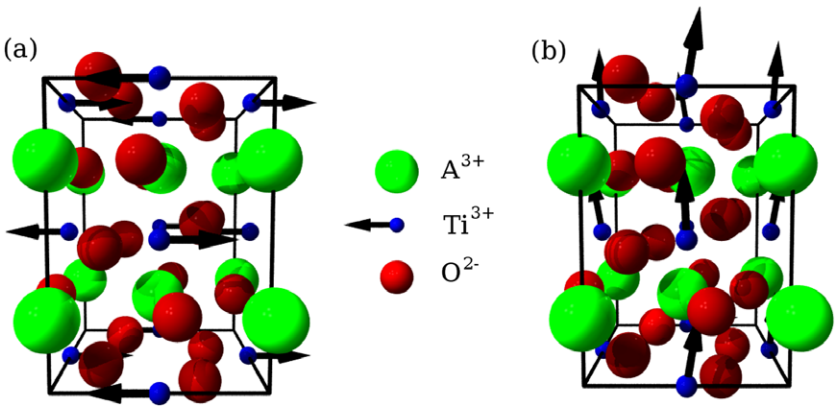

Figure 1. (a) $LaTiO_3$ and (b) $YTiO_3$, showing the magnetic structures previously proposed. Structural parameters were taken from [8] and [11], and magnetic structures from [8] and [9].

Theoretical work on these compounds has focused around the mechanism that selects the ground state from the possible spin and orbital configurations. Models considering the orbitals as quasi-static entities [3, 8, 19–21] satisfactorily predict the orbital occupation and magnetic ordering. Nevertheless, there remain aspects of the experimental observations [7, 9, 10] that cannot be successfully described without including the quantum fluctuations of the orbitals [16, 22, 23], particularly with regard to the Raman scattering results. With quasi-static orbital occupations, excitations are in the form of well-defined crystal field excitations, whereas if fluctuations are significant, the excitations are collective modes, and it is the latter which are observed by Raman scattering experiments [10]. Predicting the magnetic properties of these compounds based on their structures (i.e. the tuning provided by the A-site cation radius) and their observed orbital physics has proved challenging, particularly for $LaTiO_3$ [3]. In this context, additional detailed characterization of the magnetic properties of both compounds is worthwhile, in the hope of providing information to further constrain the theoretical models.

In this paper we describe the results of a muon spin relaxation (μSR) investigation into the magnetic properties of $LaTiO_3$ and $YTiO_3$. The methods of synthesis and the experimental details common to both compounds are explained in section 2. The results of the μSR experiments are presented in sections 3 and 4. Dipole field calculations for magnetic structures previously deduced by neutron diffraction are compared to the μSR results in section 5. The results are discussed and conclusions are drawn in section 6.

2. Experimental details

The $LaTiO_3$ sample was synthesized by arc melting appropriate mixtures of La_2O_3, TiO_2, and Ti in an argon atmosphere [24]. The properties of $LaTiO_3$ are strongly dependent on the oxygen stoichiometry (see, for examples, [10, 18]). To produce a sample as close to the correct stoichiometry as possible, several samples were prepared and one with $T_N = 135$ K, determined by magnetic measurements, was chosen. The $YTiO_3$ was prepared similarly, using Y_2O_3, and was determined to be $YTiO_{3+\delta}$ with $\delta \leqslant 0.05$, $T_C = 27$ K, and a saturation magnetic moment of 0.84 μ_B/Ti [14].

Our μSR experiments on both samples were carried out using the GPS instrument at the Paul Scherrer Institute, in zero applied magnetic field (ZF). In a μSR experiment [25] spin polarized positive muons are implanted into the sample, generally stopping at an interstitial position within the crystal structure, without significant loss of polarization. The polarization, $P_z(t)$, of the muon subsequently depends on the magnetic environment of the stopping site and can be measured using the asymmetric decay of the muon, with around 20 million muon decays recorded for each temperature point considered. The emitted positron is detected in scintillation counters around the sample position [25]. The asymmetry of the positron counts is $A(t) = (A(0) - A_{bg})P_z(t) + A_{bg}$, with $A(0) \sim 25\%$ (see figure 2) and A_{bg} a small contribution to the signal due to muons stopping outside the sample. The polycrystalline samples were wrapped in silver foil packets and mounted on a silver backing plate, since the small nuclear magnetic moment of silver minimizes the relaxing contribution of the sample mount to A_{bg}. Examples of the measured asymmetry spectra in both compounds are presented in figure 2. At low temperature, precession signals are seen in both compounds, indicative of long-range magnetic order, with two precession frequencies (see figures 3 and 4) indicating two magnetically inequivalent muon sites. Above their respective transition temperatures the data for both compounds shows exponential relaxation characteristic of a paramagnetic phase.

After the initial positron decay asymmetry, $A(0)$, and the background, A_{bg}, had been determined, preliminary fitting showed that the following equation provided a good description of the asymmetry data below the magnetic ordering temperature in each compound:

$$P_z(t) = P_f e^{-\lambda t} + P_r e^{-\sigma_r^2 t^2} + P_{osc} e^{-\sigma_{osc}^2 t^2} \times [\cos(2\pi\nu_1 t) + \cos(2\pi\nu_2 t)]. \quad (1)$$

The three components P_f, P_r, and P_{osc} are all independent of temperature. The exponentially relaxing component P_f can be attributed to fluctuating fields parallel to the direction of the implanted muon spin, since it forms approximately 1/3 of the total relaxing amplitude, as would be expected

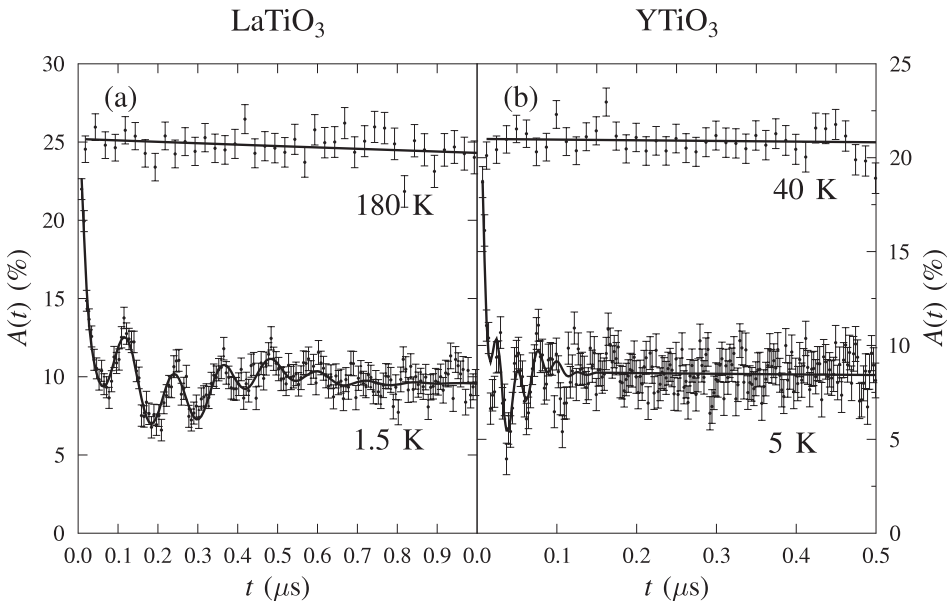

Figure 2. Examples of the raw μSR data recorded for (a) $LaTiO_3$ and (b) $YTiO_3$. For both compounds, the precession is clearly evident in the low-temperature data and absent in the high-temperature data. For the low-temperature datasets the lines plotted are fits of the data to equation (1), and for the high-temperature datasets the lines are fits to an exponential relaxation, as discussed in the text.

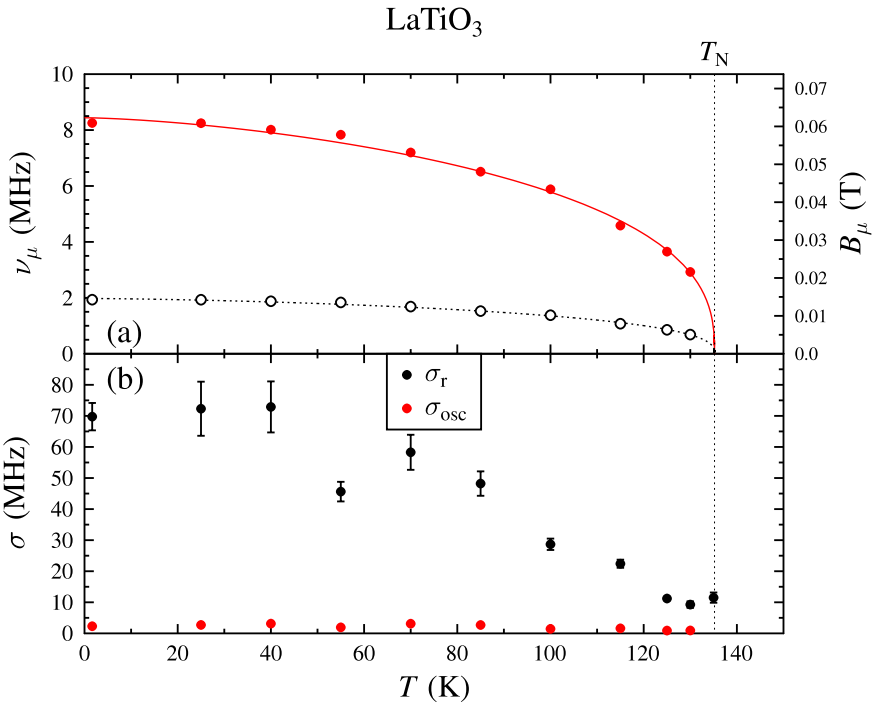

Figure 3. Parameters extracted from the raw μSR data on $LaTiO_3$ using equation (1): (a) precession frequencies ν_1 and ν_2, together with the equivalent magnetic field. (b) Gaussian relaxation rate and linewidth, σ_r and σ_{osc}. Fitted lines in (a) are to equation (2) with the parameters discussed in the text.

from polycrystalline averaging. The relaxation rate, λ, was found to be almost independent of temperature. A Gaussian relaxing component, P_r, describes the rapid drop in the asymmetry at short times, due to incoherent precession of muons stopped at sites with large and slightly inequivalent magnetic fields. The linewidths and amplitudes of the two oscillating components of P_{osc} were equal to within one standard deviation when unconstrained and therefore were set equal. The two frequencies observed are due to coherent local magnetic fields at two magnetically inequivalent muon stopping sites (we take $\nu_1 > \nu_2$). The data were fitted throughout the ordered temperature range while fixing the ratio ν_1/ν_2 to the value obtained at base temperature, consistent with the behaviour observed when their ratio was not constrained.

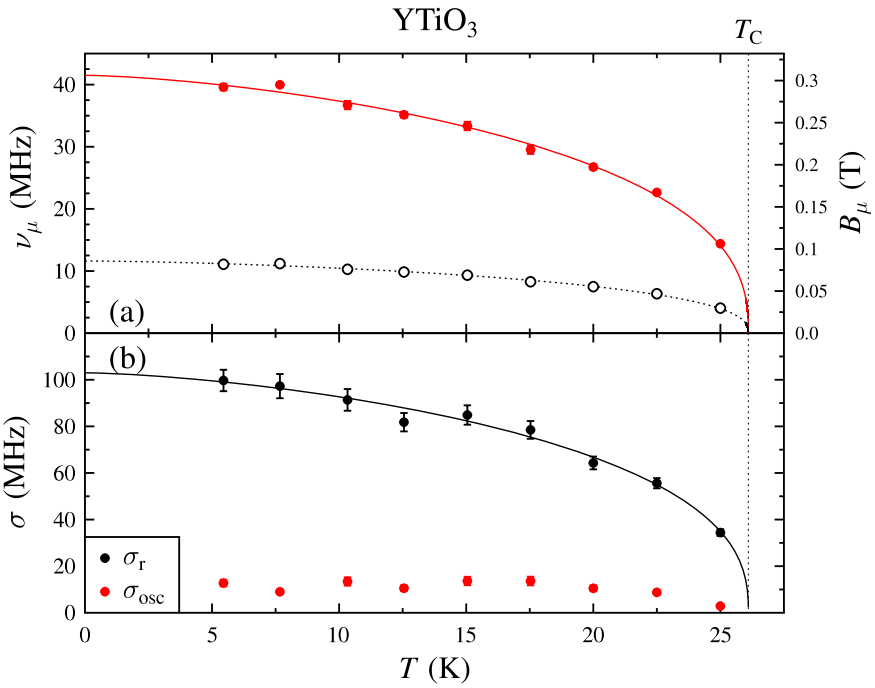

Figure 4. Parameters extracted from the raw μSR data on $YTiO_3$ using equation (1) as discussed in the text. (a) Precession frequencies ν_1 and ν_2, together with the equivalent magnetic field. (b) Gaussian relaxation rate and linewidth, σ_r and σ_{osc}. Fitted lines are to equation (2) with the parameters discussed in the text.

For both compounds the function

$$\nu_i(T) = \nu_i(0)(1 - (T/T_c)^{\alpha})^{\beta} \qquad (2)$$

was used to fit the temperature dependences of the precession frequencies $\nu_i(T)$, where T_c is the appropriate ordering temperature, α describes the temperature dependence as $T \to 0$, and β is the critical parameter describing the sublattice magnetization close to T_c [26].

3. μSR measurements on $LaTiO_3$

Raw data recorded for $LaTiO_3$ are shown in figure 2(a). The high-temperature data are well described by a single exponential relaxation consistent with fast-fluctuating electronic moments in the paramagnetic phase. Muon precession is clearly evident in the ordered phase. The fits shown in figure 2(a) were to equation (1). The ratio ν_2/ν_1 was set to 0.234 from the base temperature data. We see that the precession is rapidly damped in the ordered phase since the linewidth is comparable to the precession frequencies. The parameters obtained from fitting equation (1) to the asymmetry data, applying these constraints, are shown in figure 3.

Both precession frequencies shown in figure 3(a) are well defined up to T_N, although it was not possible to resolve a precession signal in the 135 K dataset even though the fast-relaxing component was still evident at this temperature. For $T \geqslant 140$ K, $A(t)$ took the simple exponential form expected for a fast-fluctuating paramagnetic phase. The values of ν_1 were fitted to equation (2) with $\alpha = 1.5$, leading to the parameters $\nu_1(0) = 8.4(1)$ MHz, $\beta = 0.37(3)$, and $T_N = 135(1)$ K. This value of T_N is consistent with the value found by Zhou and Goodenough [18], and it is conceivable that other magnetic studies may have been strongly affected by small regions with slightly different oxygen stoichiometry, giving the appearance of a slightly higher T_N. The linewidth of the oscillating components, σ_{osc}, is close to being temperature independent, ~2 MHz. The Gaussian relaxation rate σ_r is significantly larger than either of the precession frequencies, and roughly scales with them, suggesting that muons are stopping at sites with very large local fields, probably sitting along the magnetic moment direction of nearby Ti^{3+} ions.

4. μSR measurements on $YTiO_3$

Asymmetry spectra recorded for $YTiO_3$ are shown in figure 2(b). Again, the high-temperature data are well described by a single exponentially relaxing component, as is typical for paramagnets. Below $T_C \sim 27$ K two muon precession frequencies are again observed, consistent with long-range magnetic order developing below this temperature. Preliminary fitting showed that the amplitude of each component of equation (1) was essentially temperature independent below T_C and well defined. The ratio ν_2/ν_1 was set to the ratio at base temperature, 0.28. The fits to the data shown in figure 2(b) are to equation (1) with the parameters shown in figure 4.

The two precession frequencies shown in figure 4(a) remain in proportion for all temperatures below $T_C = 27$ K. Unlike the situation in $LaTiO_3$ however, we see that the fast-relaxing Gaussian component has a rate σ_r which follows a similar power law to the precession frequencies. In $YTiO_3$ the values of ν_1 and σ_r determined independently in the analysis

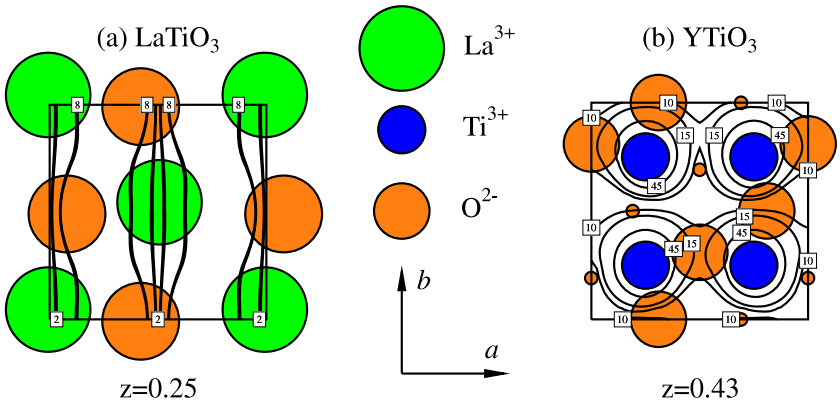

Figure 5. Examples of the results from dipole field calculations described in the text. Contours are plotted for frequencies near those observed in the μSR data and plausible sites neighbouring the O^{2-} ions ($r = 1$ Å) can be deduced. We depict the approximate radius expected with the lighter shaded area around the O^{2-} ions. (a) $LaTiO_3$ plotted in the *ab* plane with a fractional *c* coordinate of 0.25. The Ti^{3+} moments are aligned along the *a*-axis. (b) $YTiO_3$ plotted in the *ab* plane with a fractional *c* coordinate of 0.43 in the structural unit cell. A unit cell doubled along both the pseudocubic *a* and *b* axes is depicted to show the dipole field contours more clearly.

of the asymmetry data were found to be proportional to one another, in agreement with the model of muon sites with very large local fields suggested above, so both were fitted to equation (2) in parallel, fixing $\alpha = 1.5$, leading to the parameters $\nu_1(0) = 41(1)$ MHz, $\sigma_r(0) = 103(2)$ MHz, $\beta = 0.39(4)$, and $T_C = 26.0(4)$ K. The linewidth of the oscillating components is ∼10 MHz at low temperature, falling slightly towards T_C.

5. Dipole field calculations

The magnetic structures of $LaTiO_3$ and $YTiO_3$ have previously been determined using neutron scattering [7–9], although there remained some uncertainty over the orientation of the magnetic moments in $LaTiO_3$ [8]. These magnetic structures can be compared with the μSR data by calculating the dipolar fields:

$$B_{\mathrm{dip}}(\mathbf{r}_\mu) = \frac{\mu_0}{4\pi} \sum_i \frac{3(\boldsymbol{\mu}_i \cdot \hat{\mathbf{n}}_i)\hat{\mathbf{n}}_i - \boldsymbol{\mu}_i}{|\mathbf{r}_\mu - \mathbf{r}_i|^3}, \qquad (3)$$

where $\mathbf{r}_\mu$ is the position of the muon, $\boldsymbol{\mu}_i$ is the ordered magnetic moment of the *i*th Ti ion and $\hat{\mathbf{n}}_i (= (\mathbf{r}_\mu - \mathbf{r}_i)/|\mathbf{r}_\mu - \mathbf{r}_i|)$ is the unit vector from the Ti ion at site $\mathbf{r}_i$ to the muon for points within the unit cell. Contributions from of order 10^4 unit cells were considered. The resulting magnetic field distributions are periodic in $c/2$ because of the orthorhombic unit cell. Of course, this method neglects the hyperfine contact field, the Lorentz field and the demagnetizing field, although the latter two are zero for antiferromagnets and the contribution of the former to the magnetic field experienced at muon stopping sites, ∼1 Å from O^{2-} ions, is generally small. The details specific to each compound will be discussed in sections 5.1 and 5.2 below.

Such dipole field calculations have been compared to μSR data in other perovskite compounds. Some of the more thoroughly studied materials have been the rare earth orthoferrites, $RFeO_3$. The R = Sm, Eu, Dy, Ho, Y, and Er variants were studied by Holzschuh *et al* [27] and they found that the stable muon site common to all of these compounds was on the mirror plane at $z = 1/4\,(3/4)$, this being the rare earth–oxygen layer, either about 1 or 1.6 Å from the nearest oxygen ion, as would be expected for the $(OH)^-$ analogue, $(O\mu)^-$. This study was followed by others taking a slightly different approach to finding the muon sites [28, 29], and these found further plausible sites, albeit apparently metastable ones, neighbouring the rare earth–oxygen layers. Results of these studies have also been applied to orthorhombic nickelates, without precession frequencies to test the hypothesis, but the approach was consistent with phase separation occurring within magnetically inequivalent layers [30]. The most immediately relevant example within the literature is $LaMnO_3$ [31], for which a detailed study showed that the two observed precession frequencies corresponded to two structurally inequivalent muon sites, the lower frequency one within the lanthanum–oxygen mirror plane and the higher frequency one at an interstitial site within the Mn–O plane. The latter site requires a significant contribution from the contact fields due to the neighbouring oxygen ions, which the dipole field calculations presented here do not consider. Slightly earlier measurements on polycrystalline samples of $La_{1-x}Ca_xMnO_3$ were compared to dipole field calculations [32]. The same two sites, with corresponding high and low muon precession frequencies, were found for all the samples studied. In addition, there was evidence for a metastable site in $CaMnO_3$ which was not identified.

5.1. $LaTiO_3$

Dipole field calculations were carried out for the *G*-type magnetic structure reported in [7] and shown in figure 1(a). Two possible symmetry-allowed moment orientations are possible on the basis of previous neutron diffraction results, alignment along the *a*-axis or along the *c*-axis [7, 8]. Calculations were carried out for both these possible orientations with $\mu = 0.57\ \mu_B$. Representative results for $z = 1/4$ and moments aligned along the *a*-axis are shown in figure 5(a). We are looking for sites where the dipole field is close to that observed in the precession frequencies seen in

the data and the electron density is relatively large, near to the O^{2-} ions. This combination was only found to be possible for moment alignment along the a-axis. Our calculated results for moment alignment along a give very similar sites to those previously reported for the orthorhombic manganites discussed above [31, 32]. The high frequency corresponds to a site in the Ti–O layer, close to $z = 0$. As can be seen in figure 5(a), low frequency sites are found in the $z = 1/4$ plane. These are almost identical to the low-field sites reported in [31]. The contours for the higher frequency observed also pass close to oxygen atoms in the $z = 1/4$ plane but are less electrostatically favourable than the low-field sites in that layer. If sites with significantly higher local fields cause the P_r component of the observed asymmetry, these could correspond to electrostatically favourable points between O^{2-} ions in the $z = 0$ plane, with the oxygen distortions allowing magnetic inequivalency.

For the calculations carried out with the spins aligned along the c-axis it not possible to find sites in the rare earth–oxygen mirror plane at $z = 1/4$, or elsewhere within the structure, which reproduce the observed low frequency unless the O–μ distance was only ∼0.75 Å, which would be exceptionally small. Sites close to the Ti–O layer would require a significant contribution to the local field from hyperfine coupling to produce the observed precession frequencies, although this is not implausible.

Given the excellent agreement for a-axis spin alignment between the dipole field calculations at the sites previously found for a large number of compounds with this structure and the observed precession frequencies we conclude that our results strongly favour this scenario. We cannot completely exclude moment alignment along the c-axis but note that this scenario would require the muon sites to be completely different to those in all the isostructural compounds previously measured and also that no low-field sites with plausible O–μ distances were found in our calculations.

5.2. $YTiO_3$

Dipole field calculations were carried out for the ferromagnetic structure reported in [9], with moment values of $(0.106, 0.0608, 0.7034)$ μ_B along the principal axes of the pseudocubic unit cell (a, b, c), and depicted in figure 1(b). A representative slice through the structure where the contours corresponding to the observed frequencies come near to oxygen ions is shown in figure 5(b). From figure 5(b) we can see that the magnetic fields for this largely ferromagnetic structure are much larger than those in the antiferromagnetic structure of $LaTiO_3$ (figure 5(a)), in agreement with experiment. As in $LaTiO_3$ the lower frequency component in the signal is consistent with sites within the Y–O plane ($z = 1/4$), but there are no sites within this layer that would correspond to the higher frequency observed. The higher frequency component appears consistent with sites between oxygen ions near to or in the $z = 0(1/2)$ layer. Because of the small magnetic moments along the a and b-axes the contours are more distorted than those seen in $LaTiO_3$ (figure 5(a)). Considering the variation of these distortions along the c-axis leads to a structure not dissimilar to a helically ordered magnet, for these small components. This could also lead to structurally equivalent sites with much higher local fields but significant magnetic inequivalencies, leading to the fast-relaxing component, P_r, of the observed asymmetry.

6. Discussion

The μSR results clearly demonstrate intrinsic magnetic order below the expected ordering temperatures in both samples. We are also able to follow the temperature dependence of the (sub)lattice magnetization and show that the behaviour is essentially conventional. The values of β derived from equation (2) describe the behaviour close to the transition temperature. The values of $\beta = 0.37$ ($LaTiO_3$) and $\beta = 0.39$ ($YTiO_3$) are significantly below the mean field expectation of 0.5 and lie within the range 0.3–0.4 consistent with 3D critical fluctuations (e.g. 0.346 (3D XY) or 0.369 (3D Heisenberg)) [33]. This is reasonable in the context of the relatively isotropic nature of the exchange interactions in these compounds.

Our dipole field calculations described in section 5 are able to find plausible muon sites with appropriate local fields which coincide with the muon sites previously determined for rare earth orthoferrites [27–29] and orthorhombic manganites [31, 32]. For $YTiO_3$, where the magnetic structure is well known the agreement between our calculations and the observed precession frequencies is very good. Comparison between our data and calculations for the two possible moment alignments in $LaTiO_3$ strongly favours moment alignment along the a-axis. Indeed, moment alignment along the c-axis is inconsistent with the dipole field calculations. Although we have not included possible hyperfine coupling in our calculations previous results [27–29, 31] suggest it would not alter these conclusions. To determine the exact muon sites and the effect of hyperfine coupling measurements on single crystals and in applied fields would be required.

In magnetically ordered polycrystalline samples we would expect the relaxing component to account for around one third of the relaxing asymmetry, owing to the polycrystalline averaging of the effects of the magnetic fields parallel and perpendicular to the muon spin direction. The situation in these materials is not this straightforward. The fast initial relaxation σ_r is most likely to originate from large magnetic fields at muon stopping sites which are slightly magnetically inequivalent. The dipole field calculations suggest that both compounds have plausible stopping sites close to the magnetic moment directions of nearby Ti^{3+} ions, where a small range of muon stopping positions would give sufficiently different magnetic fields to lead to this fast-relaxing component.

The results presented in this paper are in excellent agreement with previous reports of the magnetic properties of both $LaTiO_3$ and $YTiO_3$ obtained using neutron diffraction [7, 9]. This confirmation is worthwhile given the history of sample dependent results and the difficulty of controlling the oxidation state precisely [10, 18]. Comparison between the precession frequencies observed in $LaTiO_3$ and dipole field calculations strongly favours moment alignment along the a-axis

rather than the *c*-axis, an issue powder neutron diffraction has difficulty resolving [8]. Using a microscopic probe gives an independent means of testing the previous results from bulk probes; our results confirm that despite the complexities of the underlying orbital physics, both compounds behave magnetically as bulk, three-dimensional magnets. We are also able to test the ability of dipole field calculations to reproduce the magnetic field distributions within oxide materials. This is successful for these compounds, where the similarity of both the structure and the muon sites nevertheless yields different internal fields due to the significantly different magnetic structures.

Acknowledgments

Part of this work was carried out at the Swiss Muon Source, Paul Scherrer Institute, Villigen, Switzerland. We thank Alex Amato for technical assistance. This research project has been supported by the EPSRC and by the European Commission under the 6th Framework Programme through the Key Action: Strengthening the European Research Area, Research Infrastructures, Contract no R113-CT-2003-505925. TL acknowledges support from the Royal Commission for the Exhibition of 1851.

References

[1] Cox P D 1992 *Transition Metal Oxides: an Introduction to Their Electronic Structure and Properties* (Oxford: Clarendon)
[2] Komarek A C, Roth H, Cwik M, Stein W-D, Baier J, Kriener M, Bourée F, Lorenz T and Braden M 2007 *Phys. Rev.* B **75** 224402
[3] Solovyev I V 2006 *Phys. Rev.* B **74** 054412
[4] Mochizuki M and Imada M 2004 *New J. Phys.* **6** 154
[5] Kusters R M, Singleton J, Keen D A, McGreevy R and Hayes W 1989 *Physica* B **155** 362
[6] Tokura Y and Nagaosa N 2000 *Science* **288** 462
[7] Keimer B, Casa D, Ivanov A, Lynn J W, Zimmermann M v, Hill J P, Gibbs D, Taguchi Y and Tokura Y 2000 *Phys. Rev. Lett.* **85** 3946
[8] Cwik M *et al* 2003 *Phys. Rev.* B **68** 060401
[9] Ulrich C, Khaliullin G, Okamoto S, Reehuis M, Ivanov A, He H, Taguchi Y, Tokura Y and Keimer B 2002 *Phys. Rev. Lett.* **89** 167202
[10] Ulrich C, Gössling A, Grüninger M, Guennou M, Roth H, Cwik M, Lorenz T, Khaliullin G and Keimer B 2006 *Phys. Rev. Lett.* **97** 157401
[11] MacLean D A, Ng H-N and Greedan J E 1979 *J. Solid State Chem.* **30** 35
[12] Haverkort M W *et al* 2005 *Phys. Rev. Lett.* **94** 056401
[13] Hemberger J *et al* 2003 *Phys. Rev. Lett.* **91** 066403
[14] Akimitsu J, Ichikawa H, Eguchi N, Miyano T, Nishi M and Kakurai K 2001 *J. Phys. Soc. Japan* **70** 3475
[15] Iga F *et al* 2004 *Phys. Rev. Lett.* **93** 257207
Iga F *et al* 2006 *Phys. Rev. Lett.* **97** 139901 (erratum)
[16] Khaliullin G and Maekawa S 2000 *Phys. Rev. Lett.* **85** 3950
[17] Kiyama T and Itoh M 2003 *Phys. Rev. Lett.* **91** 167202
[18] Zhou H D and Goodenough J B 2006 *Phys. Rev.* B **71** 184431
[19] Mochizuki M and Imada M 2003 *Phys. Rev. Lett.* **91** 167203
[20] Pavarini E, Biermann S, Poteryaev A, Lichtenstein A I, Georges A and Andersen O K 2004 *Phys. Rev. Lett.* **92** 176403
[21] Schmitz R, Entin-Wohlman O, Aharony A, Harris A B and Müller-Hartmann E 2005 *Phys. Rev.* B **71** 144412
Schmitz R, Entin-Wohlman O, Aharony A, Harris A B and Müller-Hartmann E 2007 *Phys. Rev.* B **76** 059901 (erratum)
[22] Khaliullin G and Okamoto S 2002 *Phys. Rev. Lett.* **89** 167201
[23] Khaliullin G and Okamoto S 2003 *Phys. Rev.* B **68** 205109
[24] Itoh M, Tsuchiya M, Tanaka H and Motoya K 1999 *J. Phys. Soc. Japan* **68** 2783
[25] Blundell S J 1999 *Contemp. Phys.* **40** 175
[26] Blundell S J 2001 *Magnetism in Condensed Matter Physics* (Oxford: Oxford University Press)
[27] Holzschuh E, Denison A B, Kündig W, Meier P F and Patterson B D 1983 *Phys. Rev.* B **27** 5294
[28] Boekema C, Lichti R L and Rüegg K J 1984 *Phys. Rev.* B **30** 6766
[29] Lin T K, Lichti L, Boekema C and Denison A B 1986 *Hyperfine Interact.* **31** 475
[30] García-Muñoz J L, Lacorre P and Cywinski R 1995 *Phys. Rev.* B **51** 15197
[31] Cestelli Guidi M, Allodi G, De Renzi R, Guidi G, Hennion M, Pinsard L and Amato A 2001 *Phys. Rev.* B **64** 064414
[32] Heffner R H, Sonier J E, MacLaughlin D E, Nieuwenhuys G J, Luke G M, Uemura Y J, Ratcliff W II, Cheong S-W and Balakrishnan G 2001 *Phys. Rev.* B **63** 094408
[33] Pelissetto A and Vicari E 2002 *Phys. Rep.* **368** 549